Journal of Materials Chemistry A

Exploring the Charge Reactions in Li-O2 System with Lithium Oxide Cathodes and Nonaqueous Electrolytes

Journal:	*Journal of Materials Chemistry A*
Manuscript ID	TA-COM-04-2019-003763.R1
Article Type:	Communication
Date Submitted by the Author:	31-May-2019
Complete List of Authors:	Zhang, Tao; Argonne National Laboratory, Chemical Science and Engineering Division Amine, Rachid; University of Illinois at Chicago, Chemical Engineering; Argonne National Laboratory, Materials Science Division Bi, Xuanxuan; Argonne National Laboratory, Chemical Science and Engineering Division Qin, Yan; Argonne National Laboratory, Chemical Science and Engineering Division Li, Matthew; Argonne National Laboratory, Chemical Science and Engineering Division Al-Hallaj, Said; University of Illinois at Chicago, Chemical Engineering Huo, Fengwei; Nanjing Tech University, Institute of Advanced Materials Lu, Jun; Argonne National Laboratory, Chemical Science and Engineering Division Amine, Khalil; Argonne National Laboratory,

ARTICLE

Exploring the Charge Reactions in Li-O_2 System with Lithium Oxide Cathodes and Nonaqueous Electrolytes

Received 00th January 20xx,
Accepted 00th January 20xx

DOI: 10.1039/x0xx00000x

Tao Zhang[1, 3†], Rachid Amine[3†], Xuanxuan Bi[2], Yan Qin[2], Matthew Li[2], Said Al-Hallaj[3], Fengwei Huo[1*], Jun Lu[2*] and Khalil Amine[2*]

Nonaqueous lithium-oxygen batteries have attracted considerable attention due to their high energy density. Huge efforts have been made to unravel the fundamental of Li-O_2 battery chemistry. However, current Li-O_2 batteries still suffer from several unresolved problems such as the instability of the electrolytes and the sluggish oxidation of the lithium oxides during the charging process. In this work, we propose a detailed study to investigate the charge mechanism of lithium oxide materials in different electrolytes. Commercially available lithium peroxide and lithium oxide have been employed as cathodes to determine how the lithium oxides (both lithium oxide and lithium peroxide) and electrolyte change during charge. The result shows that the Li_2O_2 decomposed to lithium and oxygen; meanwhile, the electrolyte has a significant influence on Li_2O_2 decomposition. Furthermore, while most of the Li_2O participate in the side reactions with the electrolyte, some of it is found to delithiate and crumble in structure.

Introduction

Since first introduced by Abraham and Jiang,[1] the nonaqueous rechargeable Li-O_2 battery has attracted considerable attention as a potential next-generation energy storage system owing to its extremely high theoretical energy density.[2-5] Extensive efforts and significant progress have been carried out to improve the Li-O_2 cell performance by applying novel metal-based catalysts and developing new organic type electrolytes.[6-10] However, numerous challenges still need to be overcome to enable a practical rechargeable Li-O_2 cell, such as poor cycle life, low rate capability, and poor round-trip efficiency. [11-14] These challenges are closely related to the discharge and charge reaction progresses and the chemical stability between reaction intermediates, electrolyte, and carbon electrode. In-depth understanding of the dis/charging reaction mechanisms (oxygen reduction reaction, ORR and oxygen evolution reaction, OER) is helpful for the further development of Li-O_2 batteries. The discharge reaction of Li-O_2 battery has been intensively studied that during the discharge process the Li^+ containing nonaqueous solvents would react with diffused oxygen to form Li_2O_2 or Li_2O. [15,16] There are three kinds of discharge mechanisms for these two kinds of products, respectively. These are "one electron transfer process" with lithium superoxide as the intermediate and finally forming the Li_2O_2, "two electron transfer process" directly formation of Li_2O_2 and the "four electron transfer process" with a discharge product of Li_2O. [17-20]

Compared to the discharge progress, the charging process is much more complex. First of all, Li-O_2 batteries exhibited very high charge overpotentials (> 1 V), which will result in poor round-trip efficiency and substantial energy storage inefficiency.[21] Many kinds of rationally designed catalysts including carbon based material, metals, and metal oxides have been developed try to lower the charge potential. McCloskey *et al.* [22] used Au, Pt and MnO_2 as the cathode catalyst and found none of these catalysts shows better results than a carbon electrode. However, lots of other works also showed that with OER catalysts the charge overpotential can be decreased. [23-25] Besides the charging progress of lithium oxides still unclear, for charging of Li_2O_2 there is a debate on the formation of superoxide species. While, charging of Li_2O has not been studied.

Although considerable electrolytic reduction of charging overpotential can be achieved when metal or metal oxide catalyst nanoparticles are incorporated into the porous carbon cathode, the carbonate or mixed ether-carbonate based electrolytes are severely decomposed on cell discharge. Such decomposition leads to discharge products consisting of a mixture of lithium propyl dicarbonate, lithium carbonate, HCO_2Li, CO_2, C_3H_6 $(OCO_2Li)_2$, CH_3CO_2Li, etc., rather than the desired lithium peroxide, Li_2O_2.[26] Subsequent charging involved the partial decomposition of these Li-containing compounds and the resulting CO_2 and H_2O evolution, which correlates with high charge overpotential and capacity fading alongside electrolyte consumption. Recently, the effect of different types of electrolyte (such as ether-based and carbonate-based electrolytes) on the discharge reactions of the Li-O_2 cell has been investigated from both theoretical and experimental

1 Key Laboratory of Flexible Electronics (KLOFE) & Institute of Advanced Materials (IAM), Nanjing Tech University (NanjingTech), 30 South Puzhu Road, Nanjing 211816, P. R. China
2 Chemical Sciences and Engineering Division, Argonne National Laboratory, 9700 South Cass Avenue, Lemont, IL 60439, USA
3 Department of Chemical Engineering, The University of Illinois at Chicago, Chicago, Illinois 60607, United States
Corresponding authors' email: iamfwhuo@njtech.edu.cn.(F. H.) junlu@anl.gov (J.L.) amine@anl.gov (A.K.)

prospects, which showed strong evidence that the electrolyte plays a crucial role in the cell performance. [13, 27-29] However, the fundamental mechanism of charging lithium oxide cathodes remains elusive.[12, 30]

The goal of this work is to experimentally determine the reactions involved in charging lithium oxide cathodes in different electrolytes, including both the carbonate-based and ether-based electrolyte combined with various selected Li-containing salts. In this study, we chose the most common solvents, such as propylene carbonate (PC), tri(ethylene glycol)-substituted methyltrimethyl silane (1NM3) and tetraethylene glycol dimethyl ether (TEGDME) with Li-containing salts as representative systems of interest. Several techniques, including *in-situ* high-energy X-ray diffraction (HE-XRD), X-ray photoelectron spectroscopy (XPS) and differential electrochemical mass spectrometry (DEMS) were carried out to investigate the fundamental charging process of lithium oxides. Understanding the mechanism of the charge chemistry and identification of the charge products would help predict ways to discover novel catalysts to facilitate the oxygen evolution reaction and to develop new electrolytes to achieve good rechargeability and round trip efficiency for Li-O_2 cells.

Experimental

Preparation of the cathode and electrochemical measurements:
The electrochemical cells used to investigate the decomposition of lithium oxides (Li_2O_2 and Li_2O) on charges were based on a Swagelok design and composed of a lithium metal anode, electrolytes impregnated into a glass fiber separator, and a porous cathode (11 mm in diameter). The cathode was prepared by casting a mixture of commercial Li_2O_2 (Li_2O) powder, lab-made MnO_2 nanopowders[30], Super P Li carbon and Kynar 2801 binder in a weight ratio of 1:1:1 on a carbon paper. The cells were sealed except for the Al grid window that exposed the porous cathode to 1 bar Ar/He pressure to avoid any negative effects of humidity and CO_2. The electrochemical measurements were conducted with a MACCOR cycler in the voltage range of 2.0-4.5 V at a constant current of 0.05 mA/cm^2. We normalized the observed capacity by the weight of carbon and catalyst, as practiced in other publications.[31, 32] The electrochemical characterization of Li-O_2 battery was carried out using a Swagelok-type cell composed of a lithium metal anode, a glass fiber separator impregnated with ether electrolyte and a porous cathode (11 mm diameter). The cathode was formed by mixing the as-prepared MnO_2 carbon black and polyvinylpyrrolidone (PVP) binder in a ratio of 4:4:2. The active material on each cathode was about 0.5 mg. The cells were sealed in a 1 bar pure O_2 atmosphere to avoid any negative effects of humidity and CO_2. The electrochemical measurements were conducted by a MACCOR cycler under a constant current of 0.05 mA/cm^2. The observed capacity was normalized based on the weight of the active cathode material in this study.

In-situ High-energy X-ray diffraction: The in-situ XRD experiment carried out at the 11-ID-C beamline of the Advanced Photon Source (APS), Argonne National Laboratory. The X-ray wavelength was 0.107985 Å. The high-energy X-ray source at about 0.1 Å was selected for its excellent penetration capability to detect structural changes on the bulk part of the samples during the electrochemical discharge and charge. The high flux of X-ray beam at APS is a significant advantage to carry out fast experiments at one spectrum per minute, ideal for the in-situ measurements. Home-made Swagelok-type cell composed of a lithium metal anode, electrolyte (1 M LiTFSI in TEGDME impregnated into a glass fiber separator) and a porous cathode (11mm diameter) were cycled at 50 μA/cm^2 between 2 and 4.5V using a MACCOR cycler. During the electrochemical discharge and charge, a high energy X-ray hit the sample horizontally, and a 2D Perkin Elmer large area X-ray detector was used to collect the X-ray diffraction profiles utilizing a transmission mode with a speed of one spectrum per minute. The collected 2D patterns were then integrated into conventional 1D patterns (intensity vs. 2θ) for final data analysis using the Fit2d software calibrated against a CeO_2 standard.

X-ray photoelectron spectroscopy: Samples were analyzed by X-ray photoelectron spectroscopy (XPS) using a Kratos™ Axis Ultra DLD surface analysis instrument. The base pressure of the analysis chamber during these experiments was 3 x 10^{-10} torr, with operating pressures of around 1 x 10^{-9} Torr. Spectra were collected with a monochromatic Al Kα source (1486.7 eV) and a 300 x 700 micron spot size. The Al source was operated at 13 mA of emission current with the target anode set to 15 kV; the resulting power was 195 W. For survey spectra, the data were collected at a pass energy of 160 eV (fixed analyzer transmission mode), a step size of 1 eV, and a dwell time of 200 mS. High-resolution regional spectra were collected with a pass energy of 20 eV (fixed analyzer transmission mode), a step size of 0.1 eV, and a dwell time of 300 mS. For low signal-to-noise regions, multiple passes were made, and the results averaged together. Before introduction into the load-lock vacuum chamber of the XPS instrument, all air-sensitive samples were loaded into an inert transfer module interfaced with the instrument. Samples were prepared for analysis in an Ar-filled glove box, with no more than 1 ppm O_2 and 1 ppm H_2O. Nonconductive samples showed evidence of differential charging, resulting in peak shifts and broadening. Photoelectron peak positions were shifted back toward their true values, and their peak widths were minimized by flooding the samples with low-energy electrons and ions from the charge neutralizer system on the instrument. Peak position correction was further corrected by referencing the C 1s peak position of adventitious carbon for a sample (284.8 eV, *PHI Handbook of Photoelectron Spectroscopy*), and shifting all other peaks in the spectrum accordingly.
Fitting was done by using the program Casa XPS. Each relevant spectrum was fit to a Shirley type background to correct for the rising edge of backscattered electrons that shifts the baseline

higher at high binding energies. Peaks were fit as asymmetric Gaussian/Lorentzian, with 0-30 % Lorentzian character. The FWHM of all sub-peaks was constrained to 0.7-2 eV, as dictated by instrumental parameters, lifetime broadening factors, and broadening due to sample charging. With this native resolution set, peaks were added, and the best fit, using a least-squares fitting routine, was obtained while adhering to the constraints mentioned above.

Differential Electrochemical Mass Spectrometry (DEMS) Measurements: The DEMS test was built based on a purchased mass spectrometer (HPR-40, Hiden Analytical). Known volume tubings calibrated the volumes of the sample cross-space. The mass spectrometer was calibrated by the standard mixture gas of CO_2, O_2, and H_2 (2%, 5%, and 10%) in Ar. Before cell testing, ultrahigh purity Ar was purged through the system, and the cell was isolated for gas accumulation. During the cell testing, the gas generated in the cell for every 20 min was purged and injected to the mass spectrometer. The pressure of the sample cross space was recorded by a pressure transducer (PX419-USBH).

Results and discussion

In order to confirm the importance of the catalyst in the decomposition of Li_2O_2 and Li_2O, two composites of Li_2O_2/MnO_2 and Li_2O/MnO_2 nanopowders were prepared. The charge behaviors of these electrodes were investigated in cells with Li anodes and PC-based electrolytes. As shown in Figure 1a, there is a broader and lower charging platform for both Li_2O_2/MnO_2 and Li_2O/MnO_2 compared to the non-composite electrodes of Li_2O_2 and Li_2O. There may be a number of contributing factors for the large charge overpotential, such as the poor reaction kinetics of charging of Li_2O_2, the dissatisfactory electronic conductivity of Li_2O_2, and the formation of Li_2CO_3 and other byproducts during the discharge. Here, we used commercial Li_2O_2 mixed with conductive carbon black to fabricate the electrode, which have excluded the formation the Li_2CO_3 and other byproducts, and the conductive carbon black can offer adequate electronic conductivity. Then after adding MnO_2 as the catalyst, the charge potential dropped. From our results, we can clearly observe the catalytic performance of the catalyst, so we can conclude that MnO_2 is acting as electrocatalysts for both Li_2O_2 and Li_2O, enhancing the charge capacities by lowering their delithiation voltage. The results are consistent with previous reports about the effect of MnO_2 on the charge voltage and capacities of Li-O_2 batteries. [31, 34, 35]

Figure. 1b shows the voltage profiles of Li-O_2 cells tested with multiple electrolytes that contain deferent lithium-based salts to investigate the effect of salts and solvents on the electrochemical performance of Li_2O_2. Figure 1b clearly shows that the charge capacity of the cells using $LiPF_6$+PC electrolyte is much higher than that of the cells using LiTFSI+PC. This result emphasizes the importance of salt selection on the performance of Li_2O_2. Based on previous reports, [12, 13, 34] the decomposition of lithium salts used in the electrolytes could cause detrimental electrolyte decomposition. Therefore, we believe that the drastically higher charge capacity observed in the $LiPF_6$ + PC electrolyte is likely due to electrolyte decomposition.

Organic carbonate solvents, which were widely used in the early investigation of non-aqueous Li-O_2 batteries including propylene carbonate (PC), have been shown to be unstable and decomposed irreversibly at the cathode. This is consistent with our experiment result where 1NM3 as the solvent in electrolyte is indeed more stable than the propylene carbonate. However, what is interesting is that the charge capacity of the LiTFSI+1NM3/EMS is higher than others including PC, which suggests that the LiTFSI+1NM3/EMS electrolyte is even more unstable and susceptible to decomposition of the cathode during the charge. Hence, we must realize that the two major components of the organic electrolyte: the solvents and lithium salts are both equally important in the final charge process. This interaction or compatibility between the two during discharge–charge process may severely affect the electrochemical performance of the Li-O_2 cells. As a result, we may conclude that the side reaction might be the cause of the capacity increase, and the effect of the lithium salts is more critical than solvents on electrolyte decomposition during the charge of Li_2O_2. Meantime, we should also focus on the compatibility between the solvents and lithium salts.

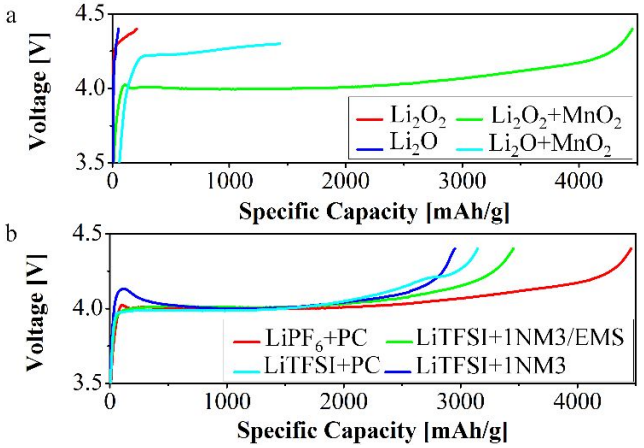

Figure 1. Voltage profiles. (a) Electrolyte: PC+1M $LiPF_6$, (b) Solvent and salt effect on the charge. Cathode: Li_2O_2+MnO_2

To further confirm that lithium oxides can be electrochemically delithiated, *in situ* XRD patterns during the charging process of Li_2O_2 and Li_2O were collected and displayed in Figure 2 and Figure 3. Figure 2 clearly shows that the Li_2O_2 peaks entirely disappeared during the charging process to 2750 mAh·g^{-1}. Therefore, we can preliminary conclude that Li_2O_2 can be successfully delithiated. More importantly, no other peaks are found, (particularly LiF peaks), which means no apparent side reactions have taken place. Therefore, it is essential to confirm that the recorded performance was indeed a measure of the electrochemical decomposition of Li_2O_2. Interestingly, when the charge capacity reached 2750 mAh·g^{-1} (LiTFSI+1NM3 sample), the Li_2O_2 had decomposed electrochemically, as shown in

Figure 2. This is further confirmation that the side reactions from electrolyte decomposition are responsible for the charge capacity increase shown in Figure 1b.

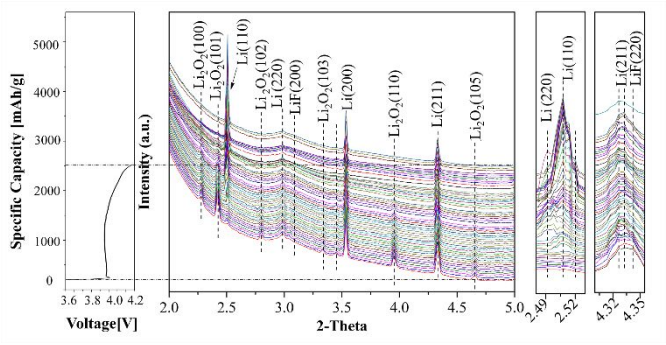

Figure 2. In-situ XRD patterns of Li_2O_2 during the charge (λ=0.107985 A). The left image is the charging curve. The two images on the right are the enlarged XRD patterns. The electrolyte is 1 M LiTFSI in TEGDME with a constant rate of 50 μA/cm².

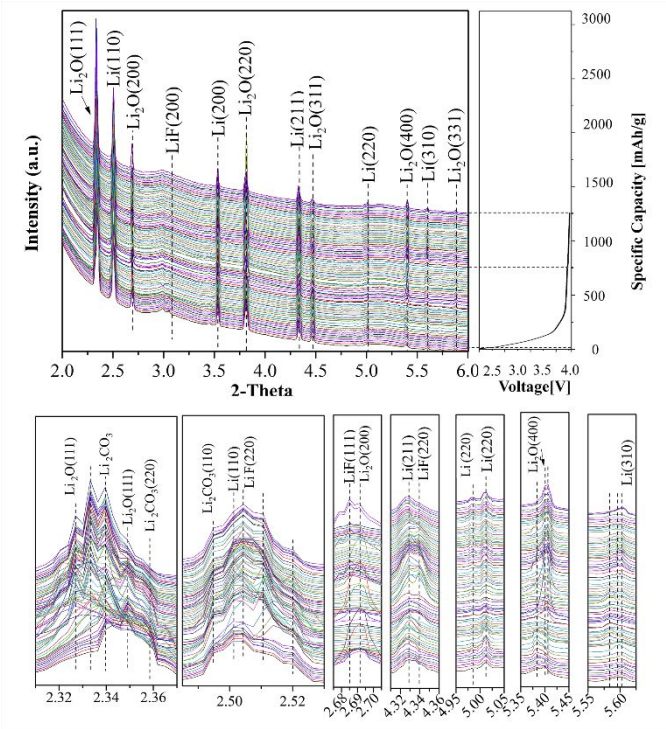

Figure 3. In-situ XRD patterns of Li_2O during the charge (λ=0.107985 A). The left image is the charging curve. The two images on the right are the enlarged XRD patterns. The electrolyte is 1 M LiTFSI in TEGDME with a constant rate of 50 μA/cm².

From Figure 3, during charging, it could be seen that the assigned peaks of Li_2O become weaker gradually but does not disappear upon charging to 1200 mAh g^{-1}. Some of the characteristic peaks of Li have also appeared which indicates that some of the Li could be charged back. At the same time, the peaks of LiF also appear, which indicate that during the charging of the Li_2O the electrolyte decomposed too, which also confirmed by the DEMS results (Figure 4c, Figure 4d). This suggests that when charged to 1200 mAh g^{-1}, only a small portion of the Li_2O would decompose to Li, while most of it remains in its pristine state, which indicates that the large charge capacity observed can be confidently attributed to the decomposition of the electrolyte.

For real-time monitoring the electrochemical decomposition of Li_2O_2 and Li_2O during the charge, DEMS measurements were conducted to detect gas generation of this process. As shown in Figure 4a, during the charging of Li_2O_2 with the LiTFSI/TEGDME, only O_2 was observed with no other gases especially the CO_2, which has a good agreement with both the *in-situ* XRD and the XPS results. On the other hand, when charging the Li_2O_2 with the carbonate-based electrolytes ($LiPF_6$ in propylene carbonate). As shown in Figure 4b, O_2 have been observed at the initial stage of the charging progress, but at later stages of the charge (4.0-4.4 V), no O_2 can be found. Instead, CO_2, which is a common byproduct of electrolyte decomposition, starts to appear. However, when the charge potential is higher than 4.4 V no O_2, and CO_2 can be detected, which indicated some parasitic reaction occurs without any detectable gas release.[11, 33] We can conclude that the PC-based electrolyte will inevitably decompose and form a variety of gases when the charge potential is higher than 4.0 V for the Li_2O containing electrode. Integrated with the in-situ XRD analysis, we can conclude that with a suitable electrolyte, the Li_2O_2 can indeed decompose to form O_2 and Li.

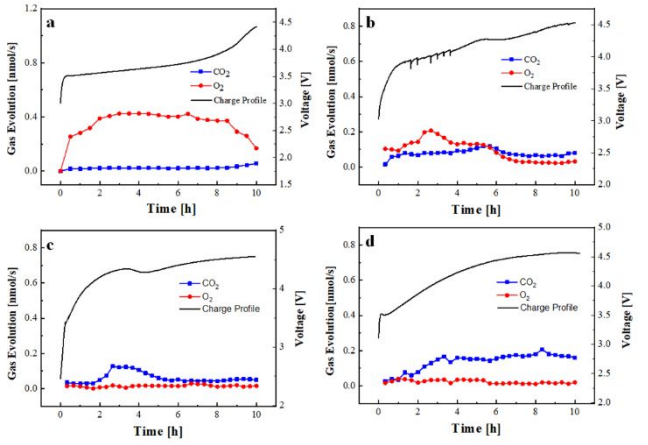

Figure 4. DEMS results of lithium oxides at different electrolytes during the charge with constant currents of 50 μA/cm² (a) Cathode: Li_2O_2+MnO_2 Electrolyte: TEGDME+1M LiTFSI, (b) Cathode: Li_2O_2+MnO_2 Electrolyte: PC+1M $LiPF_6$, (c) Cathode: Li_2O+MnO_2 Electrolyte: TEGDME+1M LiTFSI, (d) Cathode: Li_2O+MnO_2 Electrolyte: PC+1M $LiPF_6$

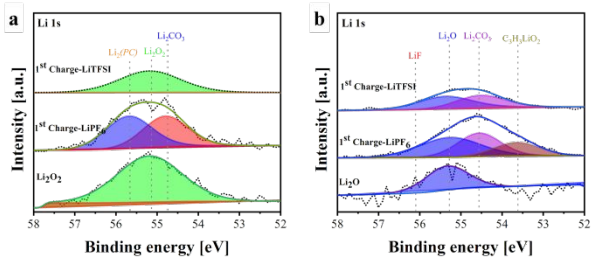

Figure 5. XPS results of lithium oxides and charged lithium oxides at different electrolytes, (a) XPS results of Li_2O_2, 1st charged in $LiPF_6$/PC and 1st charged in LiTFSI/TEGDME, (b) XPS results of Li_2O, 1st charged in $LiPF_6$/PC and 1st charged in LiTFSI/TEGDME.

However, during the charging of Li_2O electrode (Figure 4c, Figure 4d), we could not find oxygen signal in both the ether-based electrolyte and the carbonate-based electrolytes. When charging in LiTFSI/TEGDME (Figure 4c), during the first two hours no gas is detected while during the next three hours, a small amount of CO_2 is observed. Subsequent charging beyond this point has no additional gases detected. Combined with the XPS and in-situ XRD data, we can conclude that at the beginning of the charging process, part of the Li_2O contact with the catalyst did decompose into lithium, but the released oxygen intermediate did not turn into O_2 in instead of participating in side reactions with the electrolyte, causing the release of CO_2. When the electronically contacted Li_2O is depleted, the charging likely becomes just the sole reaction between the Li_2O and the electrolyte without the release of gas.[12, 36] When charging in $LiPF_6$/PC (Figure 4d), no oxygen can be detected while only CO_2 can be seen. Combined with the XPS data we propose that the whole charging progress is the decomposition of PC due to the high oxidative environment, which will cause a continuous releasing of CO_2, resulting in reactions with Li_2O to form the Li_2CO_3 and $C_3H_3LiO_2$.

To get a full picture of the charging progress of Li_2O and Li_2O_2, XPS measurements were conducted to test the surface of the electrodes both before and after charge in different electrolytes. From the Figure 5a, we can find that after charge, the peak of Li 1s is becoming weak at ~55.2 eV (Li_2O_2), and no other peaks can be found after charging, indicating that Li_2O_2 decomposes in the electrolyte of LiTFSil/TEGDM without other side reactions.[37, 38] However, when charging Li_2O_2 in the carbonate-based electrolytes ($LiPF_6$ in propylene carbonate), the peaks of Li_2CO_3 and Li_2 (PC). This indicates that some side reaction took place when charging Li_2O_2 in the $LiPF_6$/PC system.

Similarly, the XPS measurement of Li_2O and the charged products in different electrolytes have been performed. From Figure 5b, the peaks of Li_2O, Li_2CO_3, and lithium acrylates are observed, proving the formerly assumed reaction. When charged in LiTFSI/TEGDME, part of the Li_2O can decompose into lithium and a large portion will partake in side reactions, turning into lithium fluoride and Li_2CO_3, in alignment with in-situ XRD and DEMS results.

Conclusions

The investigation of the decomposition mechanism of Li_2O_2 and Li_2O is conducted, and it is confirmed that the lithium peroxides decompose to form Li and O_2 when charged in a suitable electrolyte such as some ether based electrolytes based on the *in situ* XRD, XPS and DEMS analysis. It is also found that the using of eiffient OER catalyst can significantly decrease the charge overpotential. In addition, larger capacity observed in the electrolyte solution generates large amount gaseous products (as confirmed by DEMS), suggesting that a large portion of the observed charge capacity stems directly from the decomposition of the electrolyte components. This is in stark contrast to the ideal delithiation reaction: $\boldsymbol{2Li^+ + 2e^- + O_2 \leftrightarrow Li_2O_2}$. Furthermore, the charging of Li_2O seems hard to be achieved, with most of the Li_2O participating in side reactions with the electrolyte, forming lithium fluoride, lithium carbonate, and other byproducts.

Conflicts of interest

The authors declare no competing financial interest

Acknowledgements

J. Lu and K. Amine gratefully acknowledge support from the U.S. Department of Energy (DOE), Office of Energy Efficiency and Renewable Energy, Vehicle Technologies Office. Argonne National Laboratory is operated for DOE Office of Science by UChicago Argonne, LLC, under contract number DE-AC02-06CH11357. This research used resources of the Advanced Photon Source, a U.S. Department of Energy (DOE) Office of Science User Facility operated for the DOE Office of Science by Argonne National Laboratory under Contract No. DE-AC02-06CH11357.The National Key R&D Program of China (2017YFA0207201), National Natural Science Foundation of China (21574065, 21504043, and 21604038), and the Jiangsu Provincial Funds supported this project for Natural Science Foundation (BK20160975, BK20160993. T. Zhang gratefully acknowledges the financial support from the China Scholarship Council.

Reference:

1 K.M. Abraham, Z. Jiang, *J.Electrochem. Soc.,* 1996, 143 1-5.
2 G. Girishkumar, B. McCloskey, A.C. Luntz, S. Swanson, W. Wilcke, *J. Phys. Chem. Lett.,*1 (2010) 2193-2203.
3 R. Padbury, X.W. Zhang, *J. Power Sources.,* 2011, 196 4436-4444.
4 D. Capsoni, M. Bini, S. Ferrari, E. Quartarone, P. Mustarelli, *J. Power Sources.,* 2012, 220 253-263.
5 J. Christensen, P. Albertus, R.S. Sanchez-Carrera, T. Lohmann, B. Kozinsky, R. Liedtke, J. Ahmed, A. Kojic, *J.Electrochem. Soc.,* 2012, 159 R1-R30.
6 J. Wandt, P. Jakes, J. Granwehr, H.A. Gasteiger, R.A. Eichel, *Angew. Chem. Int. Ed.,* 2016, 55 6892-6895.
7 S.M. Xu, Y.G. Yao, Y.Y. Guo, X.Q. Zeng, S.D. Lacey, H.Y. Song,

C.J. Chen, Y.J. Li, J.Q. Dai, Y.B. Wang, Y.A. Chen, B.Y. Liu, K. Fu, K. Amine, J. Lu, L.B. Hu, *Adv. Mater.*, 2018, 30.
8 M. Zhou, H.L. Wang, S.J. Guo, *Chem. Soc. Rev.*, 2016, 45 1273-1307.
9 A.C. Luntz, B.D. McCloskey, *Chem. Rev.*, 2014, 114 11721-11750.
10 Z. Jian, P. Liu, F. Li, P. He, X. Guo, M. Chen, H. Zhou, *Angew. Chem. Int. Ed.,* 2014, 53 442-446.
11 T. Liu, Z.G. Liu, G.W. Kim, J.T. Frith, N. Garcia-Araez, C.P. Grey, *Angew. Chem. Int. Ed.,* 2017, 56 16057-16062.
12 S.A. Freunberger, Y.H. Chen, Z.Q. Peng, J.M. Griffin, L.J. Hardwick, F. Barde, P. Novak, P.G. Bruce, *J. Am. Chem. Soc.,* 2011, 133 8040-8047.
13 J. Lu, L. Li, J.B. Park, Y.K. Sun, F. Wu, K. Amine, *Chem. Rev.*, 2014, 114 5611-5640.
14 V.S. Bryantsev, J. Uddin, V. Giordani, W. Walker, D. Addison, G.V. Chase, *J.Electrochem. Soc.,* 2013, 160 A160-A171.
15 Z.Y. Guo, C. Li, J.Y. Liu, Y.G. Wang, Y.Y. Xia, *Angew. Chem. Int. Ed.,* 2017, 56 7505-7509.
16 S.M. Xu, X. Liang, Z.C. Ren, K.X. Wang, J.S. Chen, *Angew. Chem. Int. Ed.,* 2018, 57 6825-6829.
17 J. Lu, Y.J. Lee, X. Luo, K.C. Lau, M. Asadi, H.-H. Wang, S. Brombosz, J. Wen, D. Zhai, Z. Chen, D.J. Miller, Y.S. Jeong, J.-B. Park, Z.Z. Fang, B. Kumar, A. Salehi-Khojin, Y.-K. Sun, L.A. Curtiss, K. Amine, *Nature*, 2016, 529 377.
18 G. Wu, N.H. Mack, W. Gao, S. Ma, R. Zhong, J. Han, J.K. Baldwin, P. Zelenay, *Acs Nano.,* 2012, 6 9764-9776.
19 J. Lu, Y. Lei, K.C. Lau, X. Luo, P. Du, J. Wen, R.S. Assary, U. Das, D. Miller, J.W. Elam, H.M. Albishri, D. Abd El-Hady, Y.-K. Sun, L.A. Curtiss, K. Amine, *Nat. Commun.,* 2014, 5.
20 C. Xia, C. Y. Kwok., L. F. Nazar. Science, 2018, 361.
21 Y.F. Yuan, K. Amine, J. Lu, R. Shahbazian-Yassar, *Nat. Commun.,* 2017,8.
22 B.D. McCloskey, R. Scheffler, A. Speidel, D. S. Bethune, A. C. Luntz,. *J. Am. Chem. Soc.* 2011, 133, 18038–18041.
23 Y.Wang, Z.Liang, Q.Zou, G.Cong, Y.C.Lu. *J. Phys. Chem. C*, 2016, 12, 6459-6466.
24 B.D. McCloskey, A. Speidel, R. Scheffler, D.C. Miller, V. Viswanathan, J.S. Hummelshoj, J.K. Norskov, A.C. Luntz, *J. Phys. Chem. Lett.*, 2012,3 997-1001.
25 Y. Chen, S.A. Freunberger, Z. Peng, F. Barde, P.G. Bruce, *J. Am. Chem. Soc.,* 2012, 134 7952-7957.
26 D. Xu, Z.L. Wang, J.J. Xu, L.L. Zhang, X.B. Zhang, *Chem. Comm.,* ,2012, 48 6948-6950.
27 J. Yi, S.H. Guo, P. He, H.S. Zhou, Energy Environ. *Sci.*, 2017, 10 860-884.
28 Z.Q. Peng, S.A. Freunberger, L.J. Hardwick, Y.H. Chen, V. Giordani, F. Barde, P. Novak, D. Graham, J.M. Tarascon, P.G. Bruce, *Angew. Chem. Int. Ed.,* 2011, 50 6351-6355.
29 B.M. Gallant, D.G. Kwabi, R.R. Mitchell, J. Zhou, C.V. Thompson, Y. Shao-Horn, Energy Environ. *Sci.*, 2013, 6 2518-2528.
30 Y. Qin, J. Lu, P. Du, Z. Chen, Y. Ren, T. Wu, J.T. Miller, J. Wen, D.J. Miller, Z. Zhang, K. Amine, Energy Environ. *Sci.*, 2013, 6 519-531.
31 X. Luo, M. Piernavieja-Hermida, J. Lu, T. Wu, J. Wen, Y. Ren, D. Miller, Z.Z. Fang, Y. Lei, K. Amine, , *Nanotechnology*, 2015, 26.
32 Y.C. Lu, Z.C. Xu, H.A. Gasteiger, S. Chen, K. Hamad-Schifferli, Y. Shao-Horn, , *J. Am. Chem. Soc.,* 2010, 132 12170-12171.
33 Y. Cao, Z. Wei, J. He, J. Zang, Q. Zhang, M. Zheng, Q. Dong, Energy Environ. *Sci.*, 2012, 5 9765-9768.
34 F. Cheng, T. Zhang, Y. Zhang, J. Du, X. Han, J. Chen, *Angew. Chem. Int. Ed.,* 2013, 52 2474-2477.
35 P. Du, J. Lu, K.C. Lau, X. Luo, J. Bareno, X. Zhang, Y. Ren, Z. Zhang, L.A. Curtiss, Y.-K. Sun, K. Amine, *Phys. Chem. Chem. Phys.,* 2013, 15, 5572-5581.
36 Y.X. Wang, P.B. Balbuena, *J. Phys. Chem. B.,* 2002, 106, 4486-4495.
37 L.M. Suo, D. Oh, Y.X. Lin, Z.Q. Zhuo, O. Borodin, T. Gao, F. Wang, A. Kushima, Z.Q. Wang, H.C. Kim, Y. Qi, W.L. Yang, F. Pan, J. Li, K. Xu, C.S. Wang, *J. Am. Chem. Soc.,* 2017, 139 18670-18680.
38 B.R. Wu, Y.H. Ren, D.B. Mu, X.J. Liu, F. Wu, *J. Power Sources.,* 2014, 272,183-189.

